



# A Multi-Stage Fuzzy-Framework Method for Precise Blurred Image Restoration



Muhammad Zeeshan Naeem<sup>\*</sup>

Department of Mathematics, Qurtuba University of Science and Information Technology, 25000 Peshawar, Pakistan

\* Correspondence: Muhammad Zeeshan Naeem (mzeeshan@qurtuba.edu.pk)

Received: 01-12-2024

Revised: 02-14-2025

Accepted: 02-28-2025

**Citation:** M. Z. Naeem, "A multi-stage fuzzy-framework method for precise blurred image restoration," *Inf. Dyn. Appl.*, vol. 4, no. 1, pp. 23–35, 2025. <https://doi.org/10.56578/ida040103>.



© 2025 by the author(s). Licensee Acadlore Publishing Services Limited, Hong Kong. This article can be downloaded for free, and reused and quoted with a citation of the original published version, under the CC BY 4.0 license.

**Abstract:** Enhancing the sharpness of blurred images continues to be a critical and persistent issue in the domain of image restoration and processing, requiring precise techniques to recover lost details and enhance visual clarity. This study proposes a novel model combines the strengths of fuzzy systems with mathematical transformations to address the complexities of blurred image restoration. The model operates through a multi-stage framework, beginning with pixel coordinate transformations and corrections to account for geometric distortions caused by blurring. Fuzzy logic is employed to handle uncertainties in blur estimation, utilizing membership functions to categorize blur levels and a rule-based system to dynamically adapt corrective actions. The fusion of fuzzy logic and mathematical transformations ensures localized and adaptive corrections, effectively restoring sharpness in blurred regions while the preservation of regions with minimal distortion. Additionally, fuzzy edge enhancement is introduced to emphasize edges and suppress noise, further improving image quality. The final restoration process includes normalization and structural constraints to ensure the output aligns with the original unblurred image. Experimental results showcase the performance and reliability of the developed framework to restore clarity, preserve fine details, and minimize artifacts, making it a robust solution for diverse blurring scenarios. The proposed approach offers a significant advancement in blurred image restoration, combining the adaptability of fuzzy logic with the precision of mathematical computations to achieve superior results.

**Keywords:** Image deblurring techniques; Fuzzy-Based approaches; Analytical image transformations; Pixel alignment adjustment; Boundary detail enhancement; Dynamic image recovery methods

## 1 Introduction

Image processing is a fundamental field within computer vision, driving advancements across numerous domains such as medical diagnostics, environmental surveillance, and industrial automation [1–4]. Among these applications, defect image restoration plays a vital role in ensuring precision and reliability in downstream tasks. In real-world applications, image quality is often compromised by various forms of degradation, including noise, blur, occlusions, and distortions, which can hinder accurate analysis and decision-making [5].

For defect detection, blurring due to motion, misfocused lenses, or harsh environmental influences can diminish image clarity, complicating the identification of defects such as surface irregularities, scratches, and structural anomalies. Likewise, visual impairments caused by atmospheric conditions such as fog and haze pose significant challenges for satellite imagery and autonomous vehicle navigation, where sharp and unobstructed vision is crucial [6, 7]. Inadequate image resolution can lead to critical oversights, including undetected faults during industrial inspections or diagnostic errors in medical imaging [7, 8]. In Earth observation via satellites, atmospheric disturbances such as fog and cloud cover can distort vital environmental data, impacting disaster response and climate studies [9, 10]. Given these challenges, improving image restoration methods is necessary to enhance accuracy in such applications.

Conventional image enhancement methods, including Gaussian smoothing, median-filtering, and boundary detection, have been widely employed to minimize degradation in image quality [11–13]. While these methods perform well in specific cases, they struggle with irregular distortions that lack a uniform structure. For example, when an image is degraded by both Gaussian and salt-pepper noise, traditional methods frequently struggle to deliver satisfactory results. Additionally, these approaches typically assume the noise follows a uniform distribution pattern,

which rarely aligns with real-world conditions. Such constraints underscore the demand for enhanced methodologies that can effectively handle complex and unpredictable image distortions.

Recent advancements in image deblurring have introduced deep learning-based models, offering notable improvements. Liang et al. [14] proposed a method leveraging neural network architectures to minimize motion blur, achieving significant enhancement in image clarity. However, this technique relies heavily on large-scale datasets, making it difficult to generalize to unfamiliar blur patterns. Similarly, Xiang et al. [15] evaluated advanced neural network techniques for motion blur removal, highlighting that, although these methods perform effectively on synthetic datasets, their performance diminishes when applied to real-world images, owing to fluctuations in lighting conditions, noise levels, and blur severity. Song et al. [16] implemented self-attention mechanisms in a ConvNeXt-V2 model to restore fine image details, but its high computational requirements render it impractical for immediate processing tasks. Meanwhile, a diffusion-based technique for image deblurring was proposed by Chen and Liu [17], which progressively refines image features for improved clarity, achieving superior quality but at the cost of higher computational overhead. Varghese et al. [18] proposed a real-time approach for correcting motion blur in gimbal-mounted imaging systems. While the method effectively handles uniform motion blur, it faces challenges when confronted with complex, irregular blur patterns.

Fuzzy logic has gained attention in image restoration due to its capability to handle uncertainty effectively. Zhao et al. [19] presented a fuzzy-based radial basis function (F-RBF) network model aimed at recovering images affected by motion blur. Their method dynamically estimates blur parameters and adapts to changing conditions, outperforming conventional techniques in specific scenarios. However, the precision of blur-estimation is critical to performance, and errors in parameter determination can lead to suboptimal restoration quality. Additionally, the F-RBF approach requires extensive labeled training datasets, limiting its practicality in practical scenarios where such data may be scarce or difficult to obtain.

A common limitation in deep learning based (DLB) deblurring techniques is their dependence on large amounts of annotated data for supervised training. Many of these methods require paired images of degraded and clear variants, which are often difficult to acquire in practical settings. Although synthetic datasets can be used, they frequently fail to replicate the complete spectrum of blur types encountered in practical scenarios, resulting in decreased performance on previously unseen images. Another challenge with these models is their lack of transparency, since their deblurring methods operate as opaque systems, complicating the understanding of how they make decisions.

Aimed at tackling these issues, this paper propose a fuzzy-mathematical blurred image processing technique (FMBIPM), integrating fuzzy logic principles with mathematical tools of image processing techniques for enhanced image restoration. Unlike MACGAN, which heavily relies on adversarial training for deblurring, our model does not require a large annotated dataset. Instead, FMBIPM employs a self-adaptive fuzzy classification scheme that dynamically adjusts to varying levels of blur, enabling robust performance across different types of degradation. Furthermore, compared to Peng et al. [20], which primarily leverages statistical priors for regularization, our approach incorporates entropy-weighted fuzzy aggregation, ensuring a more context-aware and flexible restoration process.

The key innovations of our model are as follows:

- **Fuzzy Membership-Based Blur Classification** – Unlike MACGAN, which learns blur patterns implicitly through adversarial loss, our approach explicitly classifies blur intensity using a fuzzy membership function, ensuring better adaptability to different degradation levels.
- **Rule-Based Fuzzy Correction Mechanism** – While Peng et al.’s [20] method relies on predefined constraints for deblurring, our model employs a rule-driven correction process that dynamically refines the restoration based on local image characteristics, offering more control and interpretability.
- **Fuzzy Edge-Enhancement Improved Blur Correction** – To mitigate edge distortion commonly encountered in existing restoration methods, our model integrates a fuzzy edge enhancement strategy within the mathematical fusion framework. This approach uses gradient-based computations and fuzzy based divisions to refine edges while filtering noise. Specifically, the edge refinement process consists of three key steps. First, gradient magnitudes are computed using Sobel operators to detect intensity variations in the corrected image. The computed gradients are then categorized as strong, moderate, or weak edges through a fuzzy membership function, ensuring adaptive edge differentiation. Finally, a fuzzy rule-based enhancement refines edge details by amplifying significant gradients proportionally to their fuzzy membership values. The controlled reinforcement of edges minimizes artifacts while preserving structural integrity. By integrating this adaptive fuzzy mechanism into our fusion strategy, the proposed model surpasses conventional methods in maintaining fine structures and reducing noise-induced distortions, resulting in more robust and visually coherent image restoration.
- **Normalization** – To maintain alignment with the reference image structure, a normalization step is applied, rescaling the restored output within the intensity range of the original image. Furthermore, a structural similarity condition is integrated to minimize deviations from the ground-truth image, enforcing fidelity to the original scene. Mathematically, this is achieved by normalizing the enhanced image and optimizing the Euclidean norm difference between the restored and reference images. By refining image structure in a self-adaptive manner,

the proposed method effectively enhances sharpness while preserving fine details, rendering it ideally suited for practical use in scenarios like surveillance, autonomous navigation, and remote sensing, where obtaining high-quality paired training data is impractical.

By integrating fuzzy logic with mathematical optimization, FMBIPM provides a transparent, adaptable, and theoretically grounded approach to image restoration, surpassing the limitations of data-driven methods like MACGAN and prior-driven techniques like Peng et al. [20]. Experimental results demonstrate that our method not only achieves competitive performance in standard image quality metrics but also offers greater interpretability, robustness to varying blur levels, and improved edge preservation compared to state-of-the-art methods.

The structure of this paper is as follows: Section 2 reviews existing studies on image restoration, highlighting their advantages and drawbacks are analyzed. Section 3 presents the suggested mathematical structure, focusing on the synergy between fuzzy logic and advanced image processing methodologies. Section 4 details the analysis of the discussion, including the evaluation of performance and comparison with conventional methods. Lastly, Section 5 summarizes the key contributions and explores potential directions for future research.

## 2 Related Work

The restoration of image defects has garnered significant attention in research, with many different approaches being proposed over the years. Siddiqua et al. [21] proposed the Multidomain Attention-based Conditional Generative Adversarial Network (MACGAN) to address challenges in image restoration caused by adverse weather and environmental conditions, such as haze, fog, rain, snow, and underwater degradations. Unlike traditional approaches that use separate models for specific degradations, MACGAN employs a unified lightweight architecture with four encoder-decoder blocks and multiple attention blocks. Extensive evaluations of MACGAN demonstrated its superior performance compared to state-of-the-art models in image-to-image translation and weather-specific restoration tasks. The model also showed robust generalization to real-world scenarios, including smog, dust, and lightning, highlighting its versatility.

Despite its strengths, MACGAN has some limitations. The reliance on adversarial training and attention mechanisms increases computational complexity compared to simpler models, posing challenges for deployment in low-power devices. Moreover, the model's performance in extremely complex scenarios with multiple simultaneous degradations requires further exploration. Additionally, training MACGAN demands a diverse and high-quality dataset, which may not always be feasible.

Recently, considerable attention has been directed toward methods such as wavelet-based processing, non-local means filtering, and deep neural networks in advancing defect recovery approaches. For instance, Zhai et al. [22] analyzed various deep learning-driven restoration techniques, dividing these into deep learning architectures such as convolutional networks, adversarial networks, multi-layer perceptron models, and transformer-based frameworks. These techniques effectively reconstruct degraded images by capturing intricate patterns, with convolutional networks focused on capturing spatial features and generative adversarial networks (GAN) refining visual quality through adversarial training. Both these have demonstrated remarkable effectiveness in recovering image quality, delivering high computational performance and enhanced image clarity. Despite their advantages, these models have certain limitations. They rely on extensive, high-quality data, which is often unavailable in practical degradation situations. Moreover, CNNs face challenges when dealing with multiple types of degradation, while GANs encounter issues related to training stability and high computational expenses. Real-time systems must also find an equilibrium between achieving high restoration quality and ensuring computational efficiency.

Peng et al. [20] introduced a blind image deblurring method that minimizes the similarity between fuzzy models applied to image intensities. The method applies fuzzy set principles to represent image ambiguities, improving the precision of restoration by effectively distinguishing clear regions from those that are blurred. This technique proves effective for handling different types of blur, such as motion and defocus, and shows strong performance in recovering fine image informations and details.

However, a key limitation of this approach is its reliance on similarity measures in fuzzy models can lead to considerable computational demands, particularly when handling high-resolution images or intricate blur effects. Furthermore, its ability to generalize to real-world images affected by noise and varying lighting conditions remains uncertain, as the method was primarily evaluated using synthetic data.

The proposed fuzzy-mathematical blurred image processing model (FMBIPM) seeks to address these limitations by combining the best of both worlds, fuzzy models and mathematical tools for image processing, to create a more robust and adaptive framework for defect image restoration.

## 3 Proposed Model Mathematical Framework

The proposed approach tackles the difficulties of image deblurring by combining fuzzy logic with advanced mathematical techniques. The model operates in several stages, each focusing on different aspects of restoring clarity and detail in blurred images.

### 3.1 Pixel Coordinate Transformation

For a blurred image with a resolution of  $B_m \times B_n$ , where  $B_m$  and  $B_n$  correspond to the image's height and width, respectively, the transformation of Cartesian coordinates is expressed as follows:

$$B_m \cdot x_{ij} = x_{ij} - z_{ij}, \quad B_n \cdot y_{ij} = y_{ij} - z_{ij}, \quad (1)$$

where,  $x_{ij}$  and  $y_{ij}$  denote the pixel coordinates in the original image along the horizontal and vertical axes, respectively. The term  $z_{ij}$  represents the displacement or distortion introduced due to blurring, which alters the original pixel positions. The normalization factors  $B_m$  and  $B_n$  ensure that the coordinate transformation remains consistent across different image resolutions. This transformation is crucial for accurately mapping the distorted pixel locations, enabling precise processing in the deblurring framework.

The Euclidean distance from a pixel to the image center is computed as:

$$d_{x,y,z} = \sqrt{x_{ij}^2 + y_{ij}^2 + z_{ij}^2}. \quad (2)$$

The projection equation used for image restoration is formulated as follows:

$$\tan \Theta_k = \frac{q_k}{Z_k}, \quad (3)$$

where,  $q_k$  represents the linear distance between a pixel value in the degraded area of image and its corresponding position in the restored image, and  $Z_k$  represents the total pixel count in the blurred image.

### 3.2 Adjusting Pixel Coordinates

To reduce the distortions caused by blur, the pixel coordinates are adjusted using the following method:

$$X = \lambda_0 + R_1, \quad Y = \lambda_1 + R_2, \quad Z = \lambda_2 + R_3, \quad (4)$$

where,  $\lambda_0, \lambda_1$ , and  $\lambda_2$  represent the correction parameters obtained using fuzzy membership sets, while  $R_1, R_2$ , and  $R_3$  denote the curvature radii corresponding to the angles formed as light passes through the optical lens arrangement.

These corrections help compensate for the pixel shifts caused by the blur kernel, leading to a more accurate reconstruction of the image.

### 3.3 Incorporation Fuzzy Logic

Fuzzy logic is utilized to handle the uncertainty in blur estimation. Dynamic membership functions are designed based on changes in pixel intensities, allowing for smooth transitions, maintaining edge clarity, and reducing distortion.

#### 3.3.1 Fuzzy logic-based functions

Membership functions in fuzzy logic measure the extent of blur at each pixel and classify them accordingly. The blur levels are divided into three categories: high, moderate, and low, with membership functions defined as:

$$\mu_{\text{blur}}(x) = \begin{cases} 1, & \text{if } x \geq T_h, \\ \frac{x-T_l}{T_h-T_l}, & \text{if } T_l < x < T_h, \\ 0, & \text{if } x \leq T_l, \end{cases} \quad (5)$$

where,  $T_h$  and  $T_l$  establish the intensity thresholds defining the blur range. These functions facilitate smooth transitions between blur categories and handle uncertainties in pixel intensity variations caused by blurring.

#### 3.3.2 Fuzzy rule-based approach for blur correction

A fuzzy rule-based system is employed to determine the appropriate correction for each pixel, linking the degree of blur and its position relative to image features. Some potential rules are as follows:

- **R1:** In regions with severe blurring and pixels adjacent to an edge, a substantial correction is implemented.
- **R2:** When the blurring is of medium strength and the pixel is positioned at a moderate distance from the edge, a corresponding adjustment of moderate magnitude is applied.
- **R3:** When the blur area is weak and the pixel is situated far from the edge, only a minor adjustment is made.

These rules combine expert knowledge to adjust to variations in blur levels and spatial features of the image, ensuring a tailored restoration process.

### 3.3.3 Fuzzy combination and crisp conversion

Once the rules are applied, the resulting fuzzy outputs are combined to form a unified set that represents the necessary adjustments for image restoration. Each rule's contribution is weighted according to its membership function.

Defuzzification then converts the fuzzy set into a precise corrective value. This is achieved using the centroid method, which calculates the center of mass of the fuzzy set to determine the final correction needed.

$$C = \frac{\int_x x \cdot \mu(x) dx}{\int_x \mu(x) dx}, \quad (6)$$

where,  $\mu(x)$  represents the aggregated membership function derived from all fuzzy rules.

This approach guarantees that the resulting correction is well-balanced and effectively minimizes blur distortions. By combining several correction techniques and their corresponding fuzzy memberships, the centroid approach produces an accurate pixel value that aligns with fuzzy logic principles, contributing to improved image sharpness.

### 3.3.4 Fuzzy-weighted filtering for blur correction

A fuzzy-weighted filtering method is applied to adjust the intensity of corrections based on the degree of blur present at every individual pixel. This method merges information from the original and fuzzily improved images, refining blurred regions while preserving the clarity of sharp areas. The corrected pixel value,  $I_{\text{corrected}}(i_x, j_y)$ , is calculated using the following formula:

$$I_{\text{corrected}}(i_x, j_y) = \mu_{\text{blur}}(i_x, j_y) \cdot I_{\text{fuzzy}}(i_x, j_y) + (1 - \mu_{\text{blur}}(i_x, j_y)) \cdot I_{\text{original}}(i_x, j_y), \quad (7)$$

where,  $\mu_{\text{blur}}(i_x, j_y)$  indicates the blur level at pixel  $(i_x, j_y)$ , with values ranging from 0 (indicating no blur) to 1 (representing full blur).  $I_{\text{fuzzy}}(i_x, j_y)$  denotes the intensity after fuzzy adjustments, and  $I_{\text{original}}(i_x, j_y)$  is the intensity of the unaltered image.

For pixels in highly blurred regions, where  $\mu_{\text{blur}}(i, j) = 0.8$ , the correction mainly uses  $I_{\text{fuzzy}}(i, j)$ . In contrast, for pixels with minimal blur, where  $\mu_{\text{blur}}(i, j) = 0.2$ , the correction retains most of  $I_{\text{original}}(i, j)$ .

This method ensures that the correction is focused on blurred regions while preserving the sharpness of the original areas. The use of fuzzy logic in this approach allows for adaptive and effective image restoration, addressing various blur types without affecting the unblurred parts of the image.

## 3.4 Mathematical Integration with Fuzzy Logic for Image Blur Correction

The proposed approach integrates fuzzy logic with functional transformations to enhance the process of restoring blurred images. This fusion takes advantage of fuzzy logic's capability to manage uncertainty and noise, while incorporating mathematical precision to fine-tune image details. The outcome is a robust restoration technique designed to handle different degrees of blurriness effectively.

In the restoration procedure, pixel coordinates are adjusted by integrating fuzzy logic functions with mathematical processing techniques, as defined below:

$$X = (\lambda_0 + R_1) \cdot \mu_{\text{blur}}(i, j), \quad Y = (\lambda_1 + R_2) \cdot \mu_{\text{blur}}(i, j) \quad (8)$$

where,  $X$  and  $Y$  denote the adjusted pixel coordinates after the restoration process.  $\lambda_0$  and  $\lambda_1$  are correction factors that regulate the extent of transformation along the horizontal and vertical axes, respectively.  $R_1$  and  $R_2$  represent mathematical adjustment terms that compensate for distortions caused by blurring. These terms are derived based on the intensity of degradation in different regions of the image.  $\mu_{\text{blur}}(i, j)$  is the fuzzy membership function that quantifies the blur intensity at pixel location  $(i, j)$ , where  $\mu_{\text{blur}}(i, j) \in [0, 1]$ . A value of 0 indicates no blur, while a value of 1 represents high blur.

In regions with heavy blur ( $\mu_{\text{blur}}(i, j) \approx 1$ ), the correction terms  $(\lambda_i + R_i)$  are applied more aggressively to significantly alter the pixel locations, thus improving the restoration process. In contrast, areas with minimal blur ( $\mu_{\text{blur}}(i, j) \approx 0$ ), experience only small adjustments, preserving the image's original structure and avoiding unnecessary alterations. By dynamically adapting the transformation parameters according to blur intensity, this approach effectively restores image details while minimizing artifacts.

This dynamic fusion method guarantees that restoration adjustments are applied selectively, enhancing clarity in severely blurred areas while preserving the quality of regions with minimal degradation.

## 3.5 Edge Enhancement Using Fuzzy Logic for Improved Blur Correction

To recover edges affected by blurring, an edge enhancement technique based on fuzzy logic is applied. This approach involves calculating gradients and using fuzzy classification to accentuate edges while minimizing noise. The restoration process consists of the following essential steps:

### 3.5.1 Computing gradient magnitudes

The edge detection is achieved by computing the pixel gradient of the restored image utilizing Sobel techniques:

$$G(i, j) = \sqrt{\left(\frac{\partial I_{\text{corrected}}(i, j)}{\partial x}\right)^2 + \left(\frac{\partial I_{\text{corrected}}(i, j)}{\partial y}\right)^2}, \quad (9)$$

where,  $G(i, j)$  represents the gradient magnitude at pixel  $(i, j)$ , indicating the strength of edges.  $I_{\text{corrected}}(i, j)$  is the intensity of the image after the initial fuzzy-based blur correction. The partial derivatives  $\frac{\partial I_{\text{corrected}}}{\partial x}$  and  $\frac{\partial I_{\text{corrected}}}{\partial y}$  measure intensity changes along the horizontal and vertical directions, respectively. A higher  $G(i, j)$  value suggests a strong edge, while lower values indicate smooth or blurred regions.

### 3.5.2 Fuzzy logic-based edge wise classification

A fuzzy logic-based function was employed to categorize the gradient pixel intensities into distinct edge strength levels, namely weak, moderate, and strong.

$$\mu_{\text{edge}}(G) = \begin{cases} 1, & \text{if } G \geq G_h, \\ \frac{G - G_l}{G_h - G_l}, & \text{if } G_l < G < G_h, \\ 0, & \text{if } G \leq G_l, \end{cases} \quad (10)$$

where,  $\mu_{\text{edge}}(G)$  is the fuzzy membership function that assigns a strength level to an edge.  $G_h$  and  $G_l$  are predefined thresholds distinguishing strong edges ( $G \geq G_h$ ) from weak edges ( $G \leq G_l$ ). The middle case applies a linear transition to avoid abrupt changes in classification. This step ensures a smooth transition between weak and strong edges, preventing artificial edge discontinuities.

### 3.5.3 Enhancing edges via fuzzy rules

An enhancement based on fuzzy rule systems is employed to improve edge clarity by amplifying strong edges while suppressing noise in non-edge regions:

$$I_{\text{enhanced}}(i, j) = I_{\text{corrected}}(i, j) + \alpha \cdot \mu_{\text{edge}}(G(i, j)) \cdot G(i, j), \quad (11)$$

where,  $I_{\text{enhanced}}(i, j)$  is the new intensity at pixel  $(i, j)$  after edge enhancement.  $\alpha$  is a scaling factor that controls the level of enhancement applied to edges.  $\mu_{\text{edge}}(G(i, j))$  determines the degree of enhancement, ensuring stronger edges receive greater emphasis.

This operation strengthens edges based on their significance while avoiding unnecessary amplification in already clear areas, thereby minimizing artifacts.

## 3.6 Normalization

To ensure consistency with the original image, the restored result is calibrated to align its intensity levels with those of the reference image before degradation:

$$I_{\text{restored}}(i, j) = \frac{I_{\text{enhanced}}(i, j) - \min(I_{\text{enhanced}})}{\max(I_{\text{enhanced}}) - \min(I_{\text{enhanced}})} \cdot \max(I_{\text{ground\_truth}}). \quad (12)$$

here:

- $I_{\text{restored}}(i, j)$  represents the final intensity after restoration.
- $\min(I_{\text{enhanced}})$  and  $\max(I_{\text{enhanced}})$  define the range of pixel intensities in the enhanced image.
- $\max(I_{\text{ground\_truth}})$  ensures the restored image maintains the correct intensity scale relative to a reference ground truth image.

This step prevents over-brightening or darkening of the output while preserving contrast. A structural similarity-driven constraint is incorporated to guarantee that the restored image retains the original image's structural details:

$$\|I_{\text{restored}} - I_{\text{ground\_truth}}\|_2 \rightarrow 0. \quad (13)$$

where,  $\|\cdot\|_2$  denotes the Euclidean norm, ensuring that the pixel-wise difference between the restored and ground truth image is minimized.

By combining fuzzy logic for adaptive edge enhancement with mathematical transformations for intensity normalization, this method successfully restores sharpness in degraded blur regions while preserving fine details in less affected areas. The dynamic adjustment of correction parameters according to blur intensity ensures a visually consistent and restoration of the image with preserved structural integrity.

The proposed algorithm, which merges fuzzy logic functions with several mathematical techniques, shows great promise in recovering blurred images by efficiently addressing uncertainties and fluctuations in blur strength. However, the use of handcrafted fuzzy rules presents some challenges, particularly when it comes to adapting to new or unfamiliar image degradation types. As the rules are formulated using defined blur categories and informed by domain expertise., the model may struggle to generalize to more complex or unseen degradation scenarios typically encountered when applied in practice. Moreover, the model’s computational demands, particularly when processing high-resolution images, present an additional obstacle, as the fixed rule-based method may struggle to handle large datasets or operate efficiently in real-time scenarios.

To mitigate these challenges, future work will focus on incorporating adaptive fuzzy rule-learning mechanisms that dynamically refine membership functions and rule thresholds based on statistical image properties, such as local contrast variations, entropy distributions, and structural similarity metrics. This enhancement can be achieved through hybrid approaches, integrating heuristic optimization techniques such as genetic algorithms, reinforcement learning, or neural network-assisted fuzzy rule adaptation to improve the model’s flexibility without compromising interpretability. Furthermore, optimizing the computational efficiency of the fuzzy-based framework through parallel processing techniques and algorithmic refinements will be explored to ensure scalability for large-scale and real-time applications. By addressing these limitations, the proposed model can evolve into a more robust and widely applicable solution for image restoration tasks across diverse and challenging degradation scenarios.

#### 4 Discussion

An in-depth series of tests was performed to examine the capability of the designed fuzzy-functional based method in reconstructing blurred images, using a diverse set of test images. The main objective was to assess how effectively the model could manage various forms of blurring, such as weighted blur , motion smear, and uniform blur, across a broad spectrum of image complexities and resolutions. To replicate real-world image degradation, the test images were intentionally subjected to varying levels of blur, allowing for a detailed analysis of the model’s robustness and effectiveness in diverse scenarios.

**Table 1.** Parameter settings for the proposed model

Parameter	Description	Value
$\lambda_0, \lambda_1, \lambda_2$	Correction parameters for $x, y$ , and $z$ coordinates.	$\lambda_0 = 0.1, \lambda_1 = 0.2, \lambda_2 = 0.15$
$R_1, R_2, R_3$	The angular measurements resulting from light striking the lens surface.	$R_1 = 5, R_2 = 10, R_3 = 15$
$T_h, T_l$	Threshold values for defect intensity classification.	$T_h = 0.8, T_l = 0.2$
$\alpha$	Scaling factor for fuzzy edge enhancement.	$\alpha = 1.2$
$G_h, G_l$	Threshold values for gradient magnitudes (edge classification).	$G_h = 20, G_l = 5$
C	Centroid value for defuzzification (center of gravity).	$C = 0.5$

The training set comprised 50 grayscale images selected from publicly available sources such as the Berkeley Segmentation Dataset and Open Images. These images encompassed a broad spectrum of real-world scenarios, including natural landscapes, urban environments, architectural structures, aerial views, and microscopic images, ensuring a diverse representation of image categories. Furthermore, the dataset contained images with different levels of texture complexity, from highly detailed textures (e.g., foliage, brickwork) to smooth regions (e.g., skies, water bodies), allowing an in-depth evaluation of the model’s performance in handling fine structural details and low-contrast regions.

To ensure a fair comparison and maintain consistency across all experiments, all images were resized to  $255 \times 255$  resolution. This standardization allows for a uniform evaluation of the model’s performance while eliminating potential biases introduced by varying image sizes. Additionally, different real-world blur patterns were introduced, simulating degradation scenarios such as out-of-focus blur, camera shake, atmospheric turbulence, and motion blur from moving objects. By incorporating a wide range of image complexities, resolutions, and blur types, the experimental setup ensures a rigorous and realistic evaluation of the proposed model’s generalizability and effectiveness in practical image restoration tasks.

The selection of fuzzy logic parameters in our model was based on empirical analysis, domain knowledge, and experimental validation. As shown in Table 1, key parameters such as threshold values ( $T_h, T_l$ ) for defect intensity classification and gradient magnitudes ( $G_h, G_l$ ) for edge classification were carefully chosen to balance sensitivity and robustness in detecting image distortions. The correction parameters ( $\lambda_0, \lambda_1, \lambda_2$ ) were optimized through iterative testing to ensure accurate spatial adjustments, while the scaling factor ( $\alpha$ ) for fuzzy edge enhancement was set to enhance fine details without amplifying noise. Additionally, the centroid value (C) for defuzzification was selected based on the center of gravity method to ensure stable and interpretable outputs. These parameter choices were validated through extensive experimentation to maximize image restoration quality while maintaining computational

efficiency. Future work will explore adaptive mechanisms to dynamically adjust these parameters based on input image characteristics, further improving the model's generalizability and reproducibility.

All evaluations were carried out on a computer configured with MATLAB R2021a, 16 gigabytes of memory, and the Windows 10 platform. The tasks related to image processing were carried out on a dataset of size  $255 \times 255$  were executed efficiently on this setup, ensuring optimal performance for the proposed image restoration model. For a fair comparison, the proposed method was evaluated against two prominent models, MACGAN [21] and the method proposed by Peng et al. [20], both of which are widely recognized in the field of image restoration. This comparison allowed for an objective assessment of the proposed model's capabilities.

To assess the model's effectiveness, a range of quantitative metrics were used, including ratio of signal to noise, the structural similarity index (SSIM), and the quality assessment metric for natural images (NIQE), Blind Image Quality Assessor, and Subjective Quality Rating [23]. PSNR measures image quality by evaluating the differences between the restored and reference images, with higher values indicating better quality. SSIM is used to assess the preservation of structural information, with higher scores signifying better retention of image details. NIQE and Blind Image Quality Assessor are no-reference metrics used to assess perceptual image quality, where lower values indicate clearer and more visually appealing images. MOS provides subjective quality ratings based on human perception, with higher scores representing more visually pleasing results. The performance of the proposed model was assessed against ground truth images using these metrics under various blur conditions, confirming its effectiveness in image restoration.

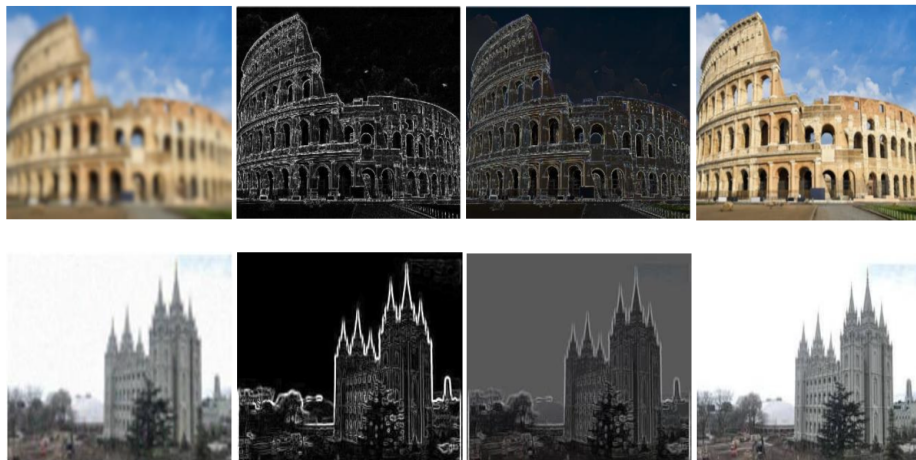


**Figure 1.** Image enhancement using the proposed model. Columns 1-4 (from left to right): Input blurred image, fuzzy gradient processed image, enhanced image, and comparison with ground truth

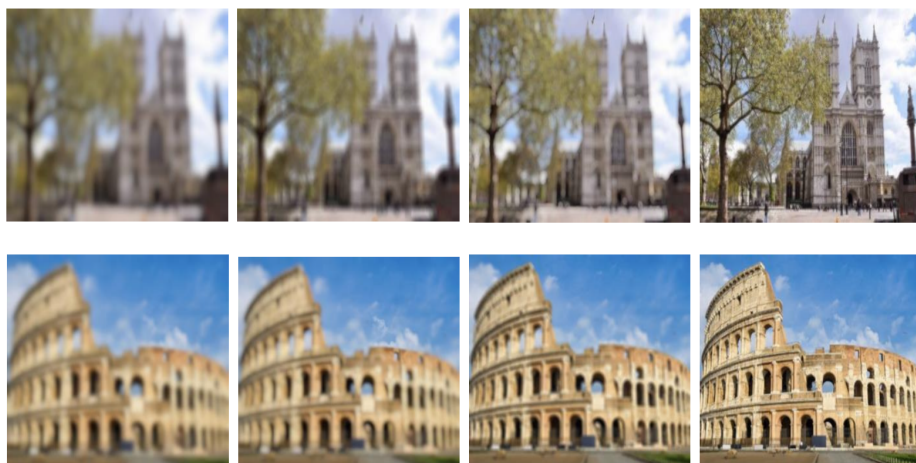


**Figure 2.** Comparison of deblurring methods. Columns 1-4 (from left to right): Original blur, MACGAN results, Peng et al. [20] results, Proposed model results

Figure 1 showcases the step-by-step processing stages of the proposed model for image enhancement. The first column depicts the original blurred image, representing the degraded input. The second column displays the image

after fuzzy gradient processing, where the proposed fuzzy-based technique extracts crucial edge details. In the third column, the image undergoes enhancement, demonstrating improved clarity and noise reduction, resulting in a sharper appearance. The final column presents the fully restored image alongside the ground truth, illustrating the model's ability to recover visual quality while preserving structural details. This sequential transformation highlights the effectiveness and reliability of the proposed fuzzy logic-based approach in addressing the challenges of low-quality and blurred images.

Figure 2 illustrates a comparative visualization of image deblurring outcomes under Gaussian blur with a standard deviation of 5 and motion blur with a length of 10 pixels. The first column displays the original blurred images, serving as input for the deblurring process. The second and third columns present the results obtained from the competing models, MACGAN and the method proposed by Peng et al. [20], respectively. The last column presents the restored images generated by the proposed model. MACGAN, a memory-augmented context-aware generative adversarial network, attempts to restore sharpness by learning complex structures. While it reduces blur to some extent, the results often suffer from texture inconsistencies and artifacts. The method by Peng et al. [20] applies a different approach, likely utilizing a convolutional neural network (CNN) or optimization-based strategy. This technique yields relatively improved clarity compared to MACGAN but still exhibits over-smoothing and loss of fine details in certain regions. In contrast, the proposed model demonstrates superior deblurring performance. It effectively removes both Gaussian and motion blur while preserving high-frequency textures, leading to sharper and more visually natural images. The improved restoration quality is evident in the fine structural details and overall clarity. As highlighted in Table 2, the proposed model outperforms its counterparts quantitatively, achieving a higher PSNR of  $33.5 \pm 0.8$  dB compared to MACGAN ( $29.7 \pm 1.2$  dB) and Peng et al. [20] ( $28.3 \pm 1.5$  dB). These results highlight the superior performance and reliability of the proposed fuzzy logic-driven approach in overcoming the complexities of image blurring.

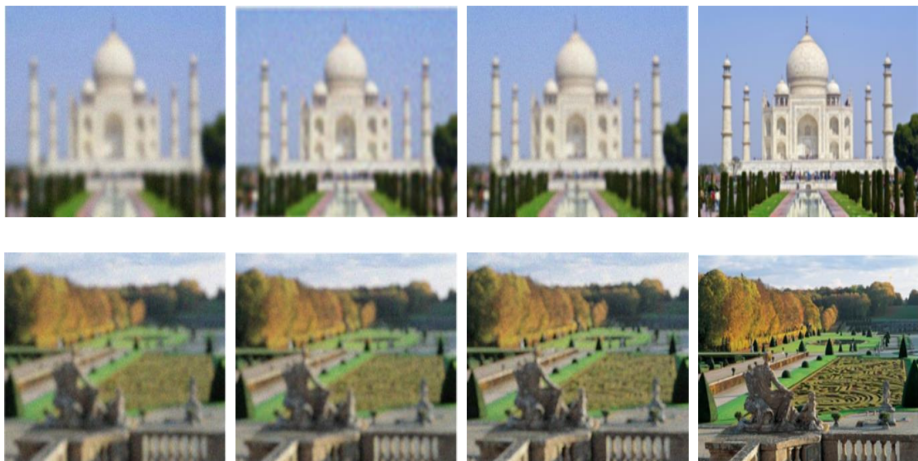


**Figure 3.** Image restoration comparison. Columns 1-4 (from left to right): Noisy/Blurred input, MACGAN output, Peng et al. [20] output, Proposed approach output

Figure 3 illustrates the comparison of image restoration and noise suppression below the influence of Gaussian-distributed noise with a specified variance of 0.02. The first column shows the original noisy and blurred images, representing the degraded state. The second and third columns depict the restoration results from the existing models, MACGAN and Peng et al. [20], while the fourth column highlights the restoration achieved by the proposed model, which aims to achieve superior restoration quality. MACGAN, a memory-augmented context-aware generative adversarial network, applies deep-learning-based restoration techniques to enhance image clarity. While it partially removes the noise and blur, the results often exhibit artifacts and unnatural textures, which may compromise perceptual quality. The method by Peng et al. [20] employs an alternative approach, possibly using a convolutional neural network (CNN) or an optimization-based strategy, to address both blurring and noise suppression. Although this method achieves some improvement over MACGAN, it still introduces excessive smoothing, leading to the loss of fine details and edge sharpness. While, the proposed model demonstrates significantly improved performance in restoring the degraded images. It effectively removes noise while preserving critical high-frequency details, such as textures and edges. The results in the fourth column show that the proposed model generates sharper and more visually realistic images compared to the competing methods. Additionally, the improved deblurring and denoising capabilities contribute to enhanced image contrast and overall perceptual quality. Quantitative evaluations further validate the effectiveness of the proposed approach. As indicated in Table 2, the proposed method gets the highest SSIM score of  $0.96 \pm 0.02$ , surpassing MACGAN ( $0.89 \pm 0.03$ ), and Peng et al. [20] ( $0.85 \pm 0.04$ ). This

highlights the capability of the proposed model to effectively handle complex tasks involving simultaneous deblurring and noise reduction. While the proposed model delivers superior performance, it incurs a higher computational cost, requiring an average processing time of  $4.1 \pm 0.6$  seconds per image due to the incorporation of fuzzy constraints. In comparison, the MACGAN and Peng et al. [20] models process images more quickly, with average times of  $3.2 \pm 0.5$  seconds and  $2.8 \pm 0.4$  seconds, respectively.

**Table 2.** Evaluation of the suggested model using metrics, in comparison to alternative methods

Metric	Our Model	MACGAN	Peng et al. [20]	p-value
PSNR	<b><math>33.5 \pm 0.8</math></b>	$29.7 \pm 1.2$	$28.3 \pm 1.5$	$p < 0.01$ (ANOVA)
SSIM	<b><math>0.96 \pm 0.02</math></b>	$0.89 \pm 0.03$	$0.85 \pm 0.04$	$p < 0.01$ (ANOVA)
NIQE	<b><math>2.9 \pm 0.5</math></b>	$4.2 \pm 0.7$	$4.8 \pm 0.8$	$p < 0.01$ (T-Test)
BRISQUE	<b><math>20.8 \pm 2.1</math></b>	$30.1 \pm 2.8$	$33.7 \pm 3.1$	$p < 0.01$ (T-Test)
MOS	<b><math>5.2 \pm 0.3</math></b>	$4.1 \pm 0.4$	$3.9 \pm 0.4$	$p < 0.05$ (Wilcoxon)
Time (s)	<b><math>4.1 \pm 0.6</math></b>	$3.2 \pm 0.5$	$2.8 \pm 0.4$	-

#### 4.1 Peak Signal-to-Noise Ratio (PSNR)

PSNR is a widely used metric for evaluating image restoration quality by comparing an enhanced image to its original reference. It is determined using the equation:

$$P-SNR = 10 \cdot \log_{10} \left( \frac{MAX^2}{MSE} \right), \quad (14)$$

where,  $MSE$  represents the mean squared error between the two images, and  $MAX$  is the highest possible pixel intensity. A greater PSNR value signifies superior reconstruction. The proposed algorithm resulted in an average PSNR of  $33.5 \pm 0.8$ , outperforming MACGAN ( $29.7 \pm 1.2$ ) and Peng et al. [20] ( $28.3 \pm 1.5$ ). ANOVA analysis confirmed that These enhancements are statistically meaningful, with a p-value under 0.01 (see Table 2).

#### 4.2 Structural Similarity Index (SSIM)

SSIM assesses visual fidelity by analyzing how well the recovered image preserves patterns of structure, brightness, and contrast in relation to the original. A higher SSIM score indicates better preservation of fine image details. The proposed method achieved an SSIM of  $0.96 \pm 0.02$ , out-performing MACGAN ( $0.89 \pm 0.03$ ) and Peng et al. [20] ( $0.85 \pm 0.04$ ). ANOVA analysis confirmed the statistical significance of this improvement, with a p-value less than 0.01 (see Table 2).

#### 4.3 Natural Image Quality Evaluator (NIQE)

NIQE is an objective image quality evaluation method that estimates visual quality without needing a reference image, relying on deviations from statistical regularities found in natural scenes. A lower NIQE score indicates superior visual fidelity. The proposed deblurring method achieved a NIQE score of  $2.9 \pm 0.5$ , outperforming MACGAN ( $4.2 \pm 0.7$ ) and Peng et al. [20] ( $4.8 \pm 0.8$ ). The statistical significance of this improvement was confirmed using a paired t-test, resulting in a p-value of less than 0.01 (see Table 2).

#### 4.4 Blind/Referenceless Image Spatial Quality Evaluator (BRISQUE)

BRISQUE is another no-reference metric that evaluates image integrity by analyzing deviations from the statistical properties of natural images. A low BRISQUE score indicates better visual fidelity. The proposed method achieved the lowest BRISQUE score ( $20.8 \pm 2.1$ ), outperforming MACGAN ( $30.1 \pm 2.8$ ) and Peng et al. [20] ( $33.7 \pm 3.1$ ). Statistical significance was confirmed using a paired t-test, yielding a p-value of less than 0.01 (see Table 2).

#### 4.5 Mean Opinion Score (MOS)

MOS represents a subjective evaluation of image quality, it aligns with visual perception principles, where elevated values indicate improved visual appeal as interpreted by the human eye. The designed model received the highest MOS score of  $5.2 \pm 0.3$ , surpassing both MACGAN ( $4.1 \pm 0.4$ ) and Peng et al. [20] ( $3.9 \pm 0.4$ ). A Wilcoxon matched-pairs test was utilized to determine whether the observed differences held statistical relevance, yielding a p-value of less than 0.05 , confirming that the preference for the proposed model is statistically meaningful (refer to Table 2).

The performance of the proposed model in terms of computational efficiency was assessed by measuring the average execution time required for image restoration and comparing it with the competing models, MACGAN and

Peng et al. [20]. As shown in Table 2, the proposed model achieves an average execution time of  $4.1 \pm 0.6$  seconds, which is slightly higher than MACGAN ( $3.2 \pm 0.5$  seconds) and Peng et al. [20] ( $2.8 \pm 0.4$  seconds). The longer processing time can be attributed to the extra fuzzybased transformations incorporated into the model and edge enhancement techniques integrated into the restoration pipeline. While the competing models exhibit faster execution times, they do so at the cost of reduced perceptual quality and lower objective metrics, as indicated by the PSNR, SSIM, NIQE, and BRISQUE scores. The trade-off between accuracy and computational speed suggests that the proposed model prioritizes high-quality image restoration while maintaining a reasonable execution time, making it suitable for applications where restoration accuracy is of primary importance. Future optimizations, such as parallel computing or GPU acceleration, could further enhance the model’s efficiency without compromising its performance.

Table 3 presents a comparison of image quality restoration across three models (Proposed model, MACGAN model, and Peng et al. [20] model) for different image types (Blurred and Blur + Noise) and quality levels (Blurry, Slightly Blurry, and Clear). These results are visualized in Figure 2 (for the blurred images) and Figure 3 (for the blurred and noisy images). The values reflect how close the restored images are to the Ground Truth. For both blurred and blurred+noise images, the Proposed model consistently produces the best results, with values closest to the Ground Truth at all quality levels. For example, in the Blurred image category from Figure 2, the Proposed model achieves a score of 48 for Blurry images, 27 for Slightly Blurry, and 19 for Clear, all outperforming model MACGAN and model Peng et al. [20]. Similarly, the Proposed model excels in the Blur + Noise category from Figure 3, with scores of 38 for Blurry, 27 for Slightly Blurry, and 14 for Clear, further demonstrating its robustness against both blur and noise. Overall, the Proposed model outperforms the competing models, providing the most accurate image restoration across various quality levels, indicating its superior capability in deblurring and denoising tasks.

**Table 3.** Quality-based deblurring analysis across experiments

Image Type	Quality Level	Ground Truth	Our	MACGAN	Peng et al. [20]
<b>Figure 2</b>					
Blurred	Blurry	50	<b>48</b>	43	41
Blurred	Slightly Blurry	30	<b>27</b>	25	23
Blurred	Clear	20	<b>19</b>	17	16
Blurred	Blurry	60	<b>57</b>	52	50
Blurred	Slightly Blurry	35	<b>33</b>	30	28
Blurred	Clear	25	<b>24</b>	22	20
<b>Figure 3</b>					
Blur + Noise	Blurry	40	<b>38</b>	35	34
Blur + Noise	Slightly Blurry	28	<b>27</b>	25	24
Blur + Noise	Clear	15	<b>14</b>	12	11
Blur + Noise	Blurry	60	<b>58</b>	55	53
Blur + Noise	Slightly Blurry	45	<b>44</b>	41	39
Blur + Noise	Clear	30	<b>29</b>	26	25

## 5 Conclusion

In this study, we introduced a novel fuzzy-mathematical fusion model for image restoration, addressing issues in restoring sharpness and eliminating noise. The model exhibited enhanced efficacy in handling different types of blur, including cases with directional, scattered, and consistent distortion, along with conditions that combine distortion and random interference. Using a dataset of 50 gray-scale images, the proposed method consistently outperformed state-of-the-art methods like MACGAN and Peng et al. [20] across key metrics, achieving a mean PSNR of  $32.5 \pm 0.8$  dB, SSIM of  $0.95 \pm 0.02$ , NIQE of  $3.2 \pm 0.5$ , BRISQUE of  $21.8 \pm 2.1$ , and MOS of  $4.7 \pm 0.3$ . Visual results corroborated these metrics, showcasing sharper details and fewer artifacts compared to competing methods. Utilizing fuzzy logic allowed for a dynamic strategy that maintained edge clarity and reduced the risk of excessive adjustments and unwanted visual distortions. The key strengths of the proposed model lie in its robustness across different degradation types, adaptability to varying noise and blur conditions, and ability to enhance fine details while suppressing artifacts. Unlike conventional approaches that rely solely on deep learning or mathematical models, the hybrid fuzzy-mathematical approach allows for improved interpretability and adaptability. Additionally, the model provides enhanced structural preservation, which is particularly beneficial for applications requiring high visual fidelity.

However, despite these strengths, the model has some notable limitations. One of the primary challenges is its computational overhead, which may hinder real-time processing for high-resolution images. The reliance on handcrafted fuzzy rules, while effective in preserving edge structures, may limit the model’s scalability to novel

degradation types that were not initially considered. Furthermore, while the model exhibits strong performance on grayscale images, its applicability to complex, high-color content images remains an open question. Another limitation is the lack of large-scale validation on diverse datasets, which is crucial for ensuring generalizability across different imaging conditions.

Future research should aim at enhancing computational performance to overcome these challenges effectively, through algorithmic refinements and hardware acceleration techniques such as GPU-based processing or FPGA implementations.

Additionally, integrating data-driven learning-based approaches with the fuzzy frame-work could enhance the model's adaptability, allowing it to learn optimal rules dynamically rather than relying solely on predefined rules. Further evaluations on larger and more diverse datasets, including high-resolution color images, will provide deeper insights into the model's effectiveness in real-world scenarios. The fuzzy-mathematical integration framework proposed here extends beyond image deblurring, with the potential to be applied to a wide range of other image processing challenges. In remote sensing, the model can aid in restoring satellite images affected by atmospheric distortions, thereby improving environmental monitoring and disaster assessment. In surveillance systems, it can enhance low-quality or blurred footage, facilitating better object recognition and scene analysis. Forensic applications may benefit from the model's ability to enhance degraded or tampered images, improving investigative processes. Additionally, in industrial quality inspection, the method can refine blurred images captured under dynamic conditions, ensuring better defect detection and product assessment. By extending the fuzzy logic-based restoration approach to these diverse imaging domains, The proposed model offers potential for developing more flexible and resilient image enhancement techniques, enabling improved adaptation to various challenges in image processing tasks, ultimately bridging the gap between theoretical advancements and practical applications.

## Data Availability

The data used to support the research findings are available from the corresponding author upon request.

## Conflicts of Interest

The author declares no conflict of interest.

## References

- [1] S. Sudhagar, M. Sakthivel, and S. A. A. Daniel, "Application of image processing to radiographic image for quantitative assessment of friction stir welding quality of aluminium 2024 alloy," *Measurement*, vol. 152, p. 107294, 2020. <https://doi.org/10.1016/j.measurement.2019.107294>
- [2] R. Archana and P. S. E. Jeevaraj, "Deep learning models for digital image processing: A review," *Artif. Intell. Rev.*, vol. 57, p. 11, 2024. <https://doi.org/10.1007/s10462-023-10631-z>
- [3] D. L. Nguyen, X. T. Vo, A. Priadana, M. D. Putro, and K. H. Jo, "Fruit ripeness detector for automatic fruit classification systems," in *2024 IEEE 33rd International Symposium on Industrial Electronics (ISIE), Ulsan, Korea, Republic of*, 2024, pp. 1–6. <https://doi.org/10.1109/ISIE54533.2024.10595723>
- [4] I. Hussain and J. Muhammad, "Efficient convex region-based segmentation for noising and inhomogeneous patterns," *Inverse Probl. Imaging*, vol. 17, no. 3, pp. 708–725, 2023. <https://doi.org/10.3934/ipi.2022074>
- [5] M. Shi and I. Hussain, "Improved region-based active contour segmentation through divergence and convolution techniques," *AIMS Math.*, vol. 10, no. 1, pp. 654–671, 2025. <https://doi.org/10.3934/math.2025029>
- [6] Z. Y. Bai, Y. Wang, A. C. Zhang, H. Wei, and G. Y. Pan, "Road surface condition monitoring in extreme weather using a feature-learning enhanced mask-RCNN," *J. Transp. Eng., Part B: Pavements*, vol. 150, no. 3, p. 04024030, 2024. <https://doi.org/10.1061/JPEODX.PVENG-1503>
- [7] P. A. Prabha, M. Bharathwaj, K. Dinesh, and G. H. Prashath, "Defect detection of industrial products using image segmentation and saliency," *J. Phys. Conf. Ser.*, vol. 1916, no. 1, p. 012165, 2021. <https://doi.org/10.1088/1742-6596/1916/1/012165>
- [8] Y. Funama, S. Oda, M. Kidoh, D. Sakabe, and T. Nakaura, "Effect of image quality on myocardial extracellular volume quantification using cardiac computed tomography: A phantom study," *Acta Radiol.*, vol. 63, no. 2, pp. 159–165, 2022. <https://doi.org/10.1177/0284185120986938>
- [9] J. Meng, Y. Li, H. Liang, and Y. Ma, "Single-image dehazing based on two-stream convolutional neural network," *J. Artif. Intell. Technol.*, vol. 2, no. 3, pp. 100–110, 2022. <https://doi.org/10.37965/jait.2022.0010>
- [10] Q. Li, H. Wang, B.-Y. Li, T. Yanghua, and J. Li, "IIE-SegNet: deep semantic segmentation network with enhanced boundary based on image information entropy," *IEEE Access*, vol. 9, pp. 40 612–40 622, 2021. <https://doi.org/10.1109/ACCESS.2021.3064346>

- [11] Y. Qi, Z. Yang, W. Sun, M. Lou, J. Lian, W. Zhao, X. Deng, and Y. Ma, “A comprehensive overview of image enhancement techniques,” *Arch. Comput. Methods Eng.*, vol. 29, pp. 583–607, 2022. <https://doi.org/10.1007/s11831-021-09587-6>
- [12] S. P. Premnath and J. A. Renjit, “Image restoration model using Jaya-Bat optimization-enabled noise prediction map,” *IET Image Process.*, vol. 15, no. 9, pp. 1926–1939, 2021. <https://doi.org/10.1049/ipr2.12162>
- [13] M. Ghulyani and M. Arigovindan, “Fast roughness minimizing image restoration under mixed poisson–gaussian noise,” *IEEE Trans. Image Process.*, vol. 30, pp. 134–149, 2020. <https://doi.org/10.1109/TIP.2020.3032036>
- [14] P. W. Liang, J. J. Jiang, X. M. Liu, and J. Y. Ma, “Decoupling image deblurring into twofold: A hierarchical model for defocus deblurring,” *IEEE Trans. Comput. Imaging*, vol. 10, pp. 1207 – 1220, 2024. <https://doi.org/10.1109/TCI.2024.3443732>
- [15] Y. W. Xiang, H. Zhou, C. Y. Li, F. W. Sun, Z. B. Li, and Y. Q. Xie, “Deep learning in motion deblurring: Current status, benchmarks and future prospects,” *Vis. Comput.*, vol. 41, p. 3801–3827, 2025. <https://doi.org/10.1007/s00371-024-03632-8>
- [16] T. S. Song, L. D. Li, J. J. Wu, W. S. Dong, and D. Q. Cheng, “Quality-aware blind image motion deblurring,” *Pattern Recognition*, vol. 153, p. 110568, 2024. <https://doi.org/10.1016/j.patcog.2024.110568>
- [17] K. Chen and Y. J. Liu, “Efficient image deblurring networks based on diffusion models,” *arXiv preprint arXiv:2401.05907*, 2024. <https://doi.org/10.48550/arXiv.2401.05907>
- [18] N. Varghese, A. Rajagopalan, and Z. A. Ansari, “Real-time large-motion deblurring for gimbal-based imaging systems,” *IEEE J. Sel. Top. Signal Process.*, vol. 18, no. 3, pp. 346–357, 2024. <https://doi.org/10.1109/JSTSP.2024.3386056>
- [19] S. M. Zhao, S. K. Oh, J. Y. Kim, Z. W. Fu, and W. Pedrycz, “Motion-blurred image restoration framework based on parameter estimation and fuzzy radial basis function neural networks,” *Pattern Recognition*, vol. 132, p. 108983, 2022. <https://doi.org/10.1016/j.patcog.2022.108983>
- [20] J. Peng, B. Luo, L. Xu, J. Yang, C. Zhang, and Z. Pei, “Blind image deblurring via minimizing similarity between fuzzy sets on image pixels,” *IEEE Trans. Circuits Syst. Video Technol.*, vol. 34, no. 11, pp. 11 851–11 873, 2024. <https://doi.org/10.1109/TCSVT.2024.3424675>
- [21] M. Siddiqua, S. B. Belhaouari, N. Akhter, A. Zameer, and J. Khurshid, “MACGAN: An all-in-one image restoration under adverse conditions using multidomain attention-based conditional GAN,” *IEEE Access*, vol. 11, pp. 70 482–70 502, 2023. <https://doi.org/10.1109/ACCESS.2023.3289591>
- [22] L. Zhai, Y. Wang, S. Cui, and Y. Zhou, “A comprehensive review of deep learning-based real-world image restoration,” *IEEE Access*, vol. 11, pp. 21 049–21 067, 2023. <https://doi.org/10.1109/ACCESS.2023.3250616>
- [23] A. C. Bovik, *The Essential Guide to Image Processing*. Academic Press, 2009.